

A New Model for Dark Matter Halos Hosting Quasars

Renyue Cen¹ and Mohammad Taher Safarzadeh²

ABSTRACT

A new model for quasar-hosting dark matter halos, meeting two physical conditions, is put forth. First, significant interactions are taken into consideration to trigger quasar activities. Second, satellites in very massive halos at low redshift are removed from consideration, due to their deficiency of cold gas. We analyze the *Millennium Simulation* to find halos that meet these two conditions and simultaneously match two-point auto-correlation functions of quasars and cross-correlation functions between quasars and galaxies at $z = 0.5 - 3.2$. The masses of found quasar hosts decrease with decreasing redshift, with the mass thresholds being $[(2-5) \times 10^{12}, (2-5) \times 10^{11}, (1-3) \times 10^{11}] M_{\odot}$ for median luminosities of $\sim [10^{46}, 10^{46}, 10^{45}] \text{erg/s}$ at $z = (3.2, 1.4, 0.53)$, respectively, an order of magnitude lower than those inferred based on halo occupation distribution modeling. In this model quasar hosts are primarily massive central halos at $z \geq 2 - 3$ but increasingly dominated by lower mass satellite halos experiencing major interactions towards lower redshift. But below $z = 1$ satellite halos in groups more massive than $\sim 2 \times 10^{13} M_{\odot}$ do not host quasars. Whether for central or satellite halos, imposing the condition of significant interactions substantially boosts the clustering strength compared to the total population with the same mass cut. The inferred lifetimes of quasars at $z = 0.5 - 3.2$ of 3–30 Myr are in agreement with observations. Quasars at $z \sim 2$ would be hosted by halos of mass $\sim 5 \times 10^{11} M_{\odot}$ in this model, compared to $\sim 3 \times 10^{12} M_{\odot}$ previously thought, which would help reconcile with the observed, otherwise puzzling high covering fractions for Lyman limit systems around quasars.

1. Introduction

Masses of dark matter halos hosting quasars are not directly measured. They are inferred by indirect methods, such as via their clustering properties (i.e., auto-correlation function, ACF, or cross-correlation function, CCF). Using ACF or CCF can yield solutions on the (lower) threshold halo masses. The solution on halo mass based on such a method is not unique, to be illustrated by a simple example. Let us suppose a sample composed of halos of large mass M and an equal number of small halos of mass m , coming in tight pairs of M and m with a separation much smaller than the scale for the correlation function of interest. For such a sample, the ACF of halos of mass M is essentially identical to that of m or cross correlation between M and m . Although dark matter halos in the standard hierarchical cold dark matter model are less simple, the feature that small

¹Princeton University Observatory, Princeton, NJ 08544; cen@astro.princeton.edu

²Johns Hopkins University, Department of Physics and Astronomy, Baltimore, MD 21218, USA

mass halos tend to cluster around massive halos is generic. This example suggests that alternative solutions of dark matter halos hosting quasars exist. It would then be of interest to find models that are based on our understanding of the thermal dynamic evolution of gas in halos and other physical considerations, which is the purpose of this *Letter*.

2. Simulations and Analysis Method

We utilize the *Millennium Simulation* (Springel et al. 2005) to perform the analysis, whose properties meet our requirements, including a large box of $500h^{-1}\text{Mpc}$, a mass resolution with dark matter particles of mass $8.6 \times 10^8 h^{-1} M_\odot$, and a spatial resolution of $5 h^{-1} \text{kpc}$ comoving. Halos are found using a *friends-of-friends* (FOF) algorithm. Satellite halos are separated out using the SUBFIND algorithm (Springel et al. 2001). The adopted ΛCDM cosmology parameters are $\Omega_m = 0.25$, $\Omega_b = 0.045$, $\Omega_\Lambda = 0.75$, $\sigma_8 = 0.9$ and $n = 1$, and $H_0 = 100h \text{ km s}^{-1} \text{ Mpc}^{-1}$ with $h = 0.73$.

Given the periodic box we compute the 2-point auto-correlation function (ACF) $\xi(r_p, \pi)$ of a halo sample by

$$\xi(r_p, \pi) = \frac{\text{DD}}{\text{RR}} - 1, \quad (1)$$

where r_p and π is the pair separation in the sky plane and along the line of sight, respectively, DD and RR are the normalized numbers of quasar-quasar and random-random pairs in each bin ($r_p - \frac{1}{2}\Delta r_p \rightarrow r_p + \frac{1}{2}\Delta r_p, \pi - \frac{1}{2}\Delta\pi \rightarrow \pi + \frac{1}{2}\Delta\pi$). The cross-correlation function (CCF) is similarly computed:

$$\xi(r_p, \pi) = \frac{D_1 D_2}{R_1 R_2} - 1, \quad (2)$$

where D_1 and D_2 correspond to galaxies and quasars. R_1 and R_2 correspond to randomly distributed galaxies and quasars that are computed analytically.

The projected 2-point correlation function $w_p(r_p)$ is: (Davis & Peebles 1983)

$$w_p(r_p) = 2 \int_0^\infty d\pi \xi_s(r_p, \pi). \quad (3)$$

In practice, the integration is up to π_{\max} . We use $\pi_{\max} = (100, 80, 70)h^{-1}\text{Mpc}$ comoving at $z = (3.2, 1.4, 0.5)$, respectively, as in observations.

3. A New Model for QSO-Hosting Dark Matter Halos at $z = 0.5 - 3.2$

Our physical modeling is motivated by insights on cosmic gas evolution from cosmological hydrodynamic simulations and observations. Simulations show four significant trends. First, cosmological structures collapse to form sheet, filaments and halos, and shock heat the gas to progressively higher temperatures with decreasing redshift (e.g., Cen & Ostriker 1999). Second, overdense regions where larger halos are preferentially located begin to be heated earlier and have higher temperatures than lower density regions at any given time, causing specific star formation rates of larger galaxies

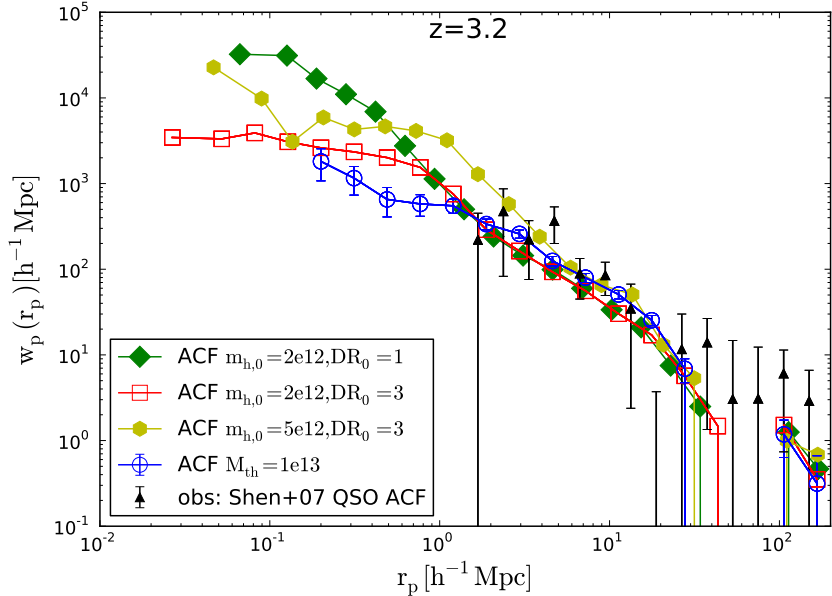


Fig. 1.— shows the ACF of quasar hosts at $z = 3.2$ for two cases of $m_{h,0} = (2 \times 10^{12}, 5 \times 10^{12}) M_\odot$ with $DR_0 = 3$ shown as (open red squares, solid yellow hexagons), respectively. For $m_{h,0} = 2 \times 10^{12} M_\odot$ one additional case is shown for $DR_0 = 1$ (solid green diamonds). For comparison, a plain threshold mass case with $M_{th} = 10^{13} M_\odot$ is shown as open blue circles. Poisson errorbars are only plotted for blue circles. Black triangles is the observed ACF (Shen et al. 2007a), using 4426 spectroscopically identified quasars at $2.9 < z < 5.4$ (median $\bar{z} = 3.2$), from the SDSS DR5 (Schneider et al. 2005; Adelman-McCarthy et al. 2006).

to fall below the general dimming trend at higher redshift than less massive galaxies and galaxies with high sSFR to gradually shift to lower density environments at lower redshift. This physical process of *differential* gravitational heating with respect to redshift is able to explain the apparent cosmic downsizing phenomenon (e.g., Cowie et al. 1996), the cosmic star formation history (e.g., Hopkins & Beacom 2006), and galaxy color migration (Cen 2011, 2014). Third, quasars appear to occur in congested environments, as evidenced by high bias inferred based on their strong clustering, with the apparent merger fraction of bright QSOs ($L > 10^{46}$ erg/s) approaching unity (e.g., Hickox et al. 2014). Finally, a quasar host galaxy presumably channels a significant amount of gas into its central black hole, which we interpret as the galaxy being rich in cold gas. This requirement would exclude satellite halos of high mass halos at lower redshift when the latter become hot gas dominated (e.g., Feldmann et al. 2011; Cen 2014). These physical considerations provide the basis for the construction of the new model detailed below in steps. First, for $z > 1$.

- (1) All - central and satellites - halos with virial mass $> m_{h,0}$ constitute the baseline sample, denoted as SA.
- (2) Each halo in SA is then selected with the following probability, $PDF(DR)$, computed as follows. For a halo X of mass m_h , we make a neighbor list of all neighbor halos with mass $\geq m_h/2$. For each neighbor halo on the neighbor list, we compute $DR_n = d_n/r_{v,n}$, where d_n is the distance from X to, and r_v is the virial radius of, the neighbor in question. We then find the minimum of all DR_n 's,

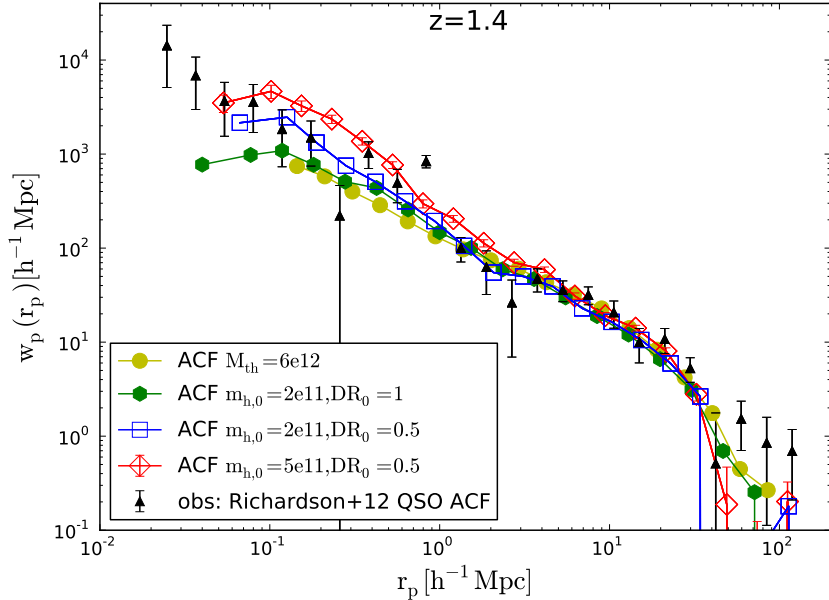


Fig. 2.— shows ACF of quasar hosts at $z = 1.4$ for three cases: $(m_{h,0}, DR_0) = (2 \times 10^{11} M_\odot, 0.5)$ (open blue squares), $(5 \times 10^{11} M_\odot, 0.5)$ (open red diamonds) and $(2 \times 10^{11} M_\odot, 1.0)$ (solid green hexagons). For comparison, a plain threshold mass case with $M_{th} = 6 \times 10^{12} M_\odot$ is shown as solid yellow circles. Poisson errorbars are only plotted for red diamonds. Black triangles are the observed ACF quasars (Richardson et al. 2012), using a sample of 47,699 quasars with a median redshift of $\bar{z} = 1.4$, drawn from the DR7 spectroscopic quasar catalog (Schneider et al. 2010; Shen et al. 2011) for large scales and 386 quasars for small scales ($< 1 \text{ Mpc/h}$) from (Hennawi et al. 2006).

calling it DR for halo X. PDF(DR) is defined as

$$\text{PDF}(DR) = 1 \quad \text{for } DR < DR_0; \quad \text{PDF}(DR) = (DR_0/DR)^3 \quad \text{for } DR \geq DR_0. \quad (4)$$

Our choice of the specific PDF is somewhat arbitrary but serves to reflect our assertion that the probability of dark matter halos hosting quasars decreases if the degree of interactions decreases, when $DR > DR_0$. The results remain little changed, for example, had we used a steeper powerlaw of 4 instead of 3. At $z < 1$, when the mean SFR in the universe starts a steep drop (Hopkins & Beacom 2006), we impose an additional criterion (3) to account for the gravitational heating.

(3) Those halos that are within the virial radius of massive halos $> M_{h,0}$ are removed, for $z < 1$.

In essence, we model the quasar hosts at $z > 1$ with two parameters, $m_{h,0}$ and DR_0 and at $z < 1$ with three parameters, $m_{h,0}$, DR_0 and $M_{h,0}$.

We present results in the order of decreasing redshift. Figure 1 shows ACF of quasar hosts at $z = 3.2$ for three cases: $(m_{h,0}, DR_0) = (2 \times 10^{12} M_\odot, 3)$, $(5 \times 10^{12} M_\odot, 3)$ and $(2 \times 10^{12} M_\odot, 1)$. Based on halo occupation distribution (HOD) modeling, Richardson et al. (2012) infer median mass of quasar host halos at $z \sim 3.2$ of $M_{cen} = 14.1_{-6.9}^{+5.8} \times 10^{12} h^{-1} M_\odot$, consistent with the threshold mass case with $M_{th} = 10^{13} M_\odot$. All model ACFs fall below the observed data at $r_p \geq 30 \text{ Mpc/h}$, due to simulation box size. The ACF amplitude is seen to increase with increasing $m_{h,0}$. The ACF with a smaller value of DR_0 steepens at a smaller r_p and rises further toward lower r_p . This

behavior is understandable, since a lower DR_0 overweights pairs at smaller separations. The extant observations do not allow useful constraints on DR_0 at $z = 3.2$. We see from visual examination that $m_{h,0} = (2 - 5) \times 10^{12} M_\odot$ provides an excellent fit to the observed ACF for $r_p = 2 - 30 h^{-1} \text{Mpc}$.

Figure 2 shows ACF of quasar hosts at $z = 1.4$ for three cases: $(m_{h,0}, DR_0) = (2 \times 10^{11} M_\odot, 0.5)$, $(5 \times 10^{11} M_\odot, 0.5)$ and $(2 \times 10^{11} M_\odot, 1.0)$. The threshold mass case with $M_{\text{th}} = 6 \times 10^{12} M_\odot$ provides a good match to the observational data for $r_p = 1 - 30 h^{-1} \text{Mpc}$, consistent with HOD modeling by Richardson et al. (2012), who constrain the median mass of the central host halos to be $M_{\text{cen}} = 4.1_{-0.4}^{+0.3} \times 10^{12} h^{-1} M_\odot$. We see that $m_{h,0} = (2 - 5) \times 10^{11} M_\odot$ provides excellent fits to the observed ACF for $r_p = 1 - 40 h^{-1} \text{Mpc}$. The observed ACF extends down to about $20 h^{-1} \text{kpc}$, which allows us to constrain DR_0 . We see that, varying DR_0 from 1.0 to 0.5, the amplitude of the ACF at $r_p \leq 1 h^{-1} \text{Mpc}$ increases, with $DR_0 = 0.5$ providing a good match. The physical implication is that quasar activities at $z = 1.4$ seem to be triggered when a halo of mass $\geq (2 - 5) \times 10^{11} M_\odot$ interact significantly with another halo of comparable mass, in contrast to the $z = 3.2$ quasars that are primarily hosted by central galaxies with no major companions.

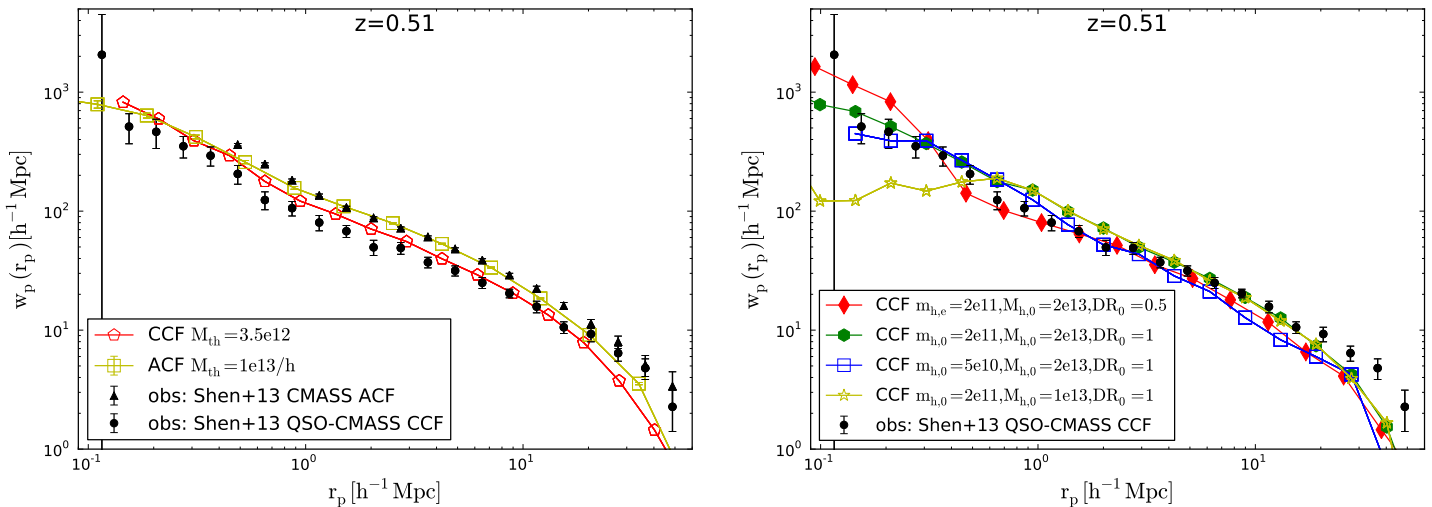


Fig. 3.— **Left panel** shows the ACF of halos of masses above $M_{\text{th}} = 1 \times 10^{13} h^{-1} M_\odot$ (open yellow squares), “mock CMASS galaxies”, and the CCF between halos of mass above $3.5 \times 10^{12} M_\odot$ and CMASS galaxies (open red pentagons). Black solid dots and triangles are the observed quasar-CMASS galaxy CCF and CMASS galaxy ACF (shown in both left and right panels), respectively, at $z \sim 0.53$ from Shen et al. (2013). The CMASS sample of 349,608 galaxies at $z \sim 0.53$ (White et al. 2011; Anderson et al. 2012) is from the Baryon Oscillation Spectroscopic Survey (Schlegel et al. 2009; Dawson et al. 2013). The sample of 8198 quasars at $0.3 < z < 0.9$ ($\langle z \rangle \sim 0.53$) is from the DR7 (Abazajian et al. 2009) spectroscopic quasar sample from SDSS I/II (Schneider et al. 2010). **Right panel** shows the model quasar-CMASS galaxy CCF at $z = 0.51$ for four cases with $(m_{h,0}, M_{h,0}, DR_0) = (2 \times 10^{11} M_\odot, 2 \times 10^{13} M_\odot, 0.5)$ (solid red diamonds), $(2 \times 10^{11} M_\odot, 2 \times 10^{13} M_\odot, 1.0)$ (solid green hexagons), $(5 \times 10^{10} M_\odot, 2 \times 10^{13} M_\odot, 1.0)$ (open blue squares) and $(2 \times 10^{11} M_\odot, 1 \times 10^{13} M_\odot, 1.0)$ (open yellow stars).

Finally, Figure 3 shows results at $z = 0.51$. The left panel shows the ACF of halos of

masses above the threshold $10^{13} h^{-1} M_\odot$ - mock CMASS galaxies - which provides a good match to the observed ACF of CMASS galaxies. Consistent with previous analysis, we see that the CCF between halos of mass above the threshold $3.5 \times 10^{12} M_\odot$ and mock CMASS galaxies match the observed counterpart. The right panel of Figure 3 shows the mock quasar-CMASS galaxy CCF at $z = 0.51$ for four cases with different combinations of $(m_{h,0}, M_{h,0}, DR_0)$. The case with $(m_{h,0}, M_{h,0}, DR_0) = [(1 - 3) \times 10^{11} M_\odot, 2 \times 10^{13} M_\odot, 0.5]$ provides an adequate match to the observation, while $(m_{h,0}, M_{h,0}, DR_0) = (5 \times 10^{10} M_\odot, 2 \times 10^{13} M_\odot, 1.0)$ appears to underestimate the CCF. The case with $(2 \times 10^{11} M_\odot, 1 \times 10^{13} M_\odot, 1.0)$ significantly underestimates the observed ACF at $r_p < 0.5 h^{-1} \text{Mpc}$. This indicates that halos of masses greater than $m_{h,0} = (1 - 3) \times 10^{11} M_\odot$ residing in environment of groups of masses $(1 - 2) \times 10^{13} M_\odot$ are primarily responsible for the strong clustering at $r_p < 0.5 h^{-1} \text{Mpc}$. It is interesting to note that the exclusion halo mass of $M_{h,0} = 2.0 \times 10^{13} M_\odot$, to account for environment heating effects, is physically self-consistent with the fact that the red CMASS galaxies are red due to the same environment effects hence have about the same halo mass ($M_{\text{th}} = 10^{13} h^{-1} M_\odot$).

4. Predictions and Tests of our Model

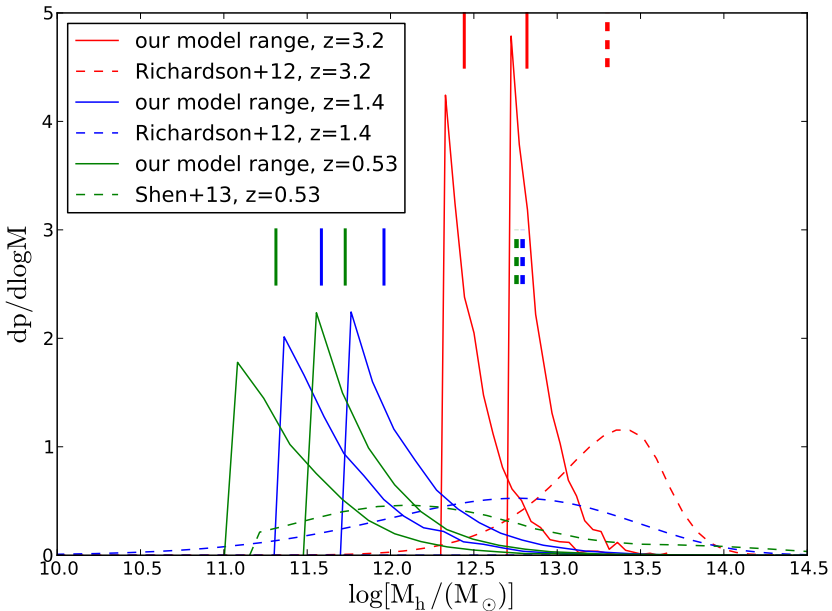


Fig. 4.— shows the QSO-hosting halo mass distributions at $z = 3.2$ (solid red curves), $z = 1.4$ (solid blue curves) and $z = 0.53$ (solid green curves). We show two bracketing (approximately $\pm 1\sigma$ for the computed correlation functions) models at each redshift. The corresponding distributions based on HOD modeling are shown in dashed curves. The short vertical bars with matching colors and line types indicate the median halo masses of their respective distributions.

We have demonstrated that our physically based model can account for the observed clustering of quasars at $z = 3.2, 1.4, 0.53$. Figure 4 contrasts the sharp differences between our model and the conventional HOD based modeling; the halo masses in our model are an order of magnitude lower than those inferred from HOD modeling. Our model gives quasar-hosting halo mass threshold of

$[(2 - 5) \times 10^{12}, (2 - 5) \times 10^{11}, (1 - 3) \times 10^{11}] M_{\odot}$ at $z = (3.2, 1.4, 0.53)$, respectively. compared to median mass of $(14.1^{+5.8}_{-6.9} \times 10^{12}, 4.1^{+0.3}_{-0.4} \times 10^{12}, 4.0 \times 10^{12}) h^{-1} M_{\odot}$ based on HOD modeling (Richardson et al. 2012; Shen et al. 2013). Although we have not made fitting for quasars at redshift higher than $z = 3.2$, we anticipate that the quasars at higher redshifts that have comparable luminosities as those at $z = 3.2$ will primarily be hosted by central galaxies of mass $\sim (2 - 5) \times 10^{12} M_{\odot}$. We note that the median luminosity of the observed quasars decreases from $\sim 10^{46} \text{ erg/s}$ at $z \geq 1.4$ to $\sim 10^{45} \text{ erg/s}$ at $z = 0.53$, which reflects the known downsizing scenario and is in accord with the decreasing halo mass with decreasing redshift inferred in our model. Our results and detailed comparisons with HOD based modeling are also tabulated in Table 1, along with inferred quasar duty cycles and lifetimes.

Can we differentiate between these two models? Trainor & Steidel (2012) cross correlate 1558 galaxies with spectroscopic redshifts with 15 of the most luminous ($\geq 10^{14} L_{\odot}$, $M_{1450} \sim -30$) quasars at $z \sim 2.7$. Even for these hyperluminous quasars (HLQSOs), they infer host halo mass of $\log(M_h/M_{\odot}) = 12.3 \pm 0.5$, which is in very good agreement with our model ($M_h \sim (2 - 5) \times 10^{12} M_{\odot}$) but much smaller than inferred from HOD modeling. They also find that, on average, the HLQSOs lie within significant galaxy over-densities, characterized by a velocity dispersion $\sigma_v \sim 200 \text{ km/s}$ and a transverse angular scale of $\sim 25''$ (~ 200 physical kpc), which they argue correspond to small groups with $\log(M_h/M_{\odot}) \sim 13$. The rare HLQSOs are apparently not hosted by rare dark matter halos. This is fully consistent with our suggestion that dark matter halo mass is not the sole determining factor of quasar luminosities and that interactions may be instrumental to triggering quasar activities.

Another, independent method to infer halo masses of quasar hosts is to measure their cold gas content. Prochaska et al. (2013) detect about 60% – 70% covering fraction of Lyman limit systems within the virial radius of $z \sim 2$ quasars, using the binary quasar sample (Hennawi et al. 2006). This has created significant tension: hydrodynamic simulations of the cold dark matter model yield less than 20% covering fraction for halos of mass $\sim 3 \times 10^{12} M_{\odot}$ (Faucher-Giguere et al. 2014); halos of still higher mass have still lower covering fractions. On the other hand, the simulations show a $\sim 60\%$ covering fraction if the mass of quasar-hosting halos is $\sim 3 \times 10^{11} M_{\odot}$. This indicates that the lower halo masses for quasar hosts in our model can explain the high content of neutral gas in $z \sim 2$ quasars.

The mean quasar lifetime may be estimated by equating it to $t_H \times f_q$, where t_H is the Hubble time at the redshift in question and f_q the duty cycle of quasar hosting halos. Existing observational constraints provide useful range for t_q for quasars at $z \sim 3$. Lifetimes based on halo abundances from clustering analyses of quasars have been given by many authors (e.g., Martini & Weinberg 2001; Porciani et al. 2004; Shen et al. 2007b); in our case, this is a degenerate derivation. Thus, it is useful to have a survey of quasar lifetimes based on other, independent methods. Jakobsen et al. (2003) derive $t_q > 10 \text{ Myr}$, Worseck et al. (2007) give $t_q > 25 \text{ Myr}$, Gonçalves et al. (2008) yield $t_q = 16 - 33 \text{ Myr}$, and McQuinn & Worseck (2014) yield $t_q > 10 \text{ Myr}$ for quasars at $z \approx 2 - 3$, all based on the method of quasar proximity effect. Bolton et al. (2012) obtain $t_q > 3 \text{ Myr}$ using line-of-sight thermal proximity effect. Trainor & Steidel (2013), using a novel method of Ly α emitters (LAEs) exhibiting fluorescent emission via the reprocessing of ionizing radiation from

nearby hyperluminous QSOs, find $1 \leq t_q \leq 20$ Myr at $z = 2.5 - 2.9$. We see that all these estimates are consistent with our model. As a comparison, the inferred $t_q^{\text{HOD}} \sim 400$ Myr at $z = 3.2$ from HOD modeling.

Finally, self-consistently reproducing the quasar luminosity functions (e.g., Wyithe & Loeb 2002, 2003; Shen 2009; Conroy & White 2013) will provide another test, which we defer to a separate study.

Table 1: Comparing Our Model With HOD Modeling w.r.t. Halo Mass and Quasar Lifetime

(1) z_{med}	(2) L_{bol} $\log(\frac{\text{erg}}{\text{s}})$	(3) n_{obs} $\times 10^{-7}$	(4) n_{sim} $\times 10^{-4}$	(5) $m_{h,0}$ $\times 10^{12}$	(6) f_q $\times 10^{-3}$	(7) t_q [Myr]	(8) M_h^{HOD} $\times 10^{12}$	(9) f_q^{HOD} $\times 10^{-3}$	(10) t_q^{HOD} [Myr]
3.2	46.3	2.5	0.2 – 0.9	2 – 5	3 – 13	5-26	20	215	425
1.4	46.1	30	9 – 44	0.2 – 0.5	0.6 – 3	3-15	5.8	1.8	7.5
0.53	45.1	50	29 – 85	0.1 – 0.3	0.6 – 2	5-15	5.7	1.3	10

Column (1) z_{med} is the median redshift of the sample that is analyzed.

Column (2) L_{bol} is the median bolometric luminosity of the observed quasar sample obtained using conversions in (Richards et al. 2006; Runnoe et al. 2012).

Column (3) n_{obs} is the number density of the observed quasar sample (Shen & Kelly 2012) in [$\text{Mpc}^3 h^{-3}$], multiplied by a factor of 2.5 to account for the fact that about 60% of quasars belong to the so-called type II quasars based on low redshift observations (Zakamska et al. 2003), which are missed in the quoted observational sample. We note that the percentage of obscured quasars appear to increase with redshift (e.g., Ballantyne et al. 2006; Treister & Urry 2006). Thus, the values of t_q may be underestimated.

Column (4) $m_{h,0}$ is the lower mass threshold dark matter halos hosting quasars in [M_\odot].

Column (5) n_{sim} is the number density of the dark matter halos hosting quasars with mass $\geq m_{h,0}$ in [$\text{Mpc}^{-3} h^3$].

Column (6) $f_q \equiv n_{\text{obs}}/n_{\text{sim}}$ is the duty cycle of the quasars in our model.

Column (7) t_q is the mean quasar lifetime in our model defined as $t_H \times f_q$, where t_H is the Hubble time at the redshift in question.

Column (8) $M_{h,\text{med}}^{\text{HOD}}$ is the derived host halo mass of the observed population of quasars derived from HOD modeling (Richardson et al. 2012; Shen et al. 2013) in [M_\odot].

Column (9) f_q^{HOD} is the duty cycle of the observed population of quasars based on HOD modeling, using the type II quasars-corrected abundance in Column (3).

Column (10) t_q^{HOD} is the life time of the quasars based on f_q^{HOD} in Column (9).

5. Conclusions

We put forth new model for dark matter halos that host quasars. Our model is substantially different from previous models based on simple lower mass threshold or HOD based lower mass threshold. Instead, we impose two conditions that are physically based. First condition is that significant interactions with other halos are a necessary ingredient to trigger quasar activities.

Second, satellite halos within the virial radius of large halos above certain mass at low redshift are removed from consideration, since they are hot gas dominated. We investigate this model utilizing halo catalogs from the *Millennium Simulation*. By requiring simultaneously that halos meet these two conditions and match two-point auto-correlation functions of quasars and cross-correlation functions between quasars and galaxies, we are able to identify quasar hosting halos. The resulting host halos are distinctly different from other models. Quasar hosts are less massive, by an order of magnitude, than inferred based on either simple halo mass threshold or HOD models. The lower halo mass threshold of quasar hosts are predicted to be $[(2-5) \times 10^{12}, (2-5) \times 10^{11}, (1-3) \times 10^{11}] M_{\odot}$ at $z = (3.2, 1.4, 0.53)$, respectively, compared to median mass of $(14.1_{-6.9}^{+5.8} \times 10^{12}, 4.1_{-0.4}^{+0.3} \times 10^{12}, 4.0 \times 10^{12}) h^{-1} M_{\odot}$ based on HOD modeling. It is noted that, for either central or satellite halos, imposing the condition of significant interactions substantially boosts the clustering strength compared to the total population with the same mass cut, which is the reason why our lower mass halos can equally well match observed clustering of quasars. At $z \geq 2$ the quasar hosts are primarily central galaxies and major interactions at close separations do not appear to be necessary, whereas at $z < 2$ the quasar hosts mostly are satellite galaxies which experience major interactions to trigger the quasar activities. Below $z = 1$ satellite galaxies in groups of mass $\geq 2 \times 10^{13} M_{\odot}$ do not host quasars due to lack of cold gas. The mean quasar lifetime is, nearly invariably, expected to be in the range of 3 – 30 Myr for the redshift range examined $z = 0.5 - 3.2$, which is in good agreement with observations. A unique and discriminatory property is that, unlike other previous models, the quasar hosting galaxies in this model are expected to be cold gas rich and have much higher covering fractions for Lyman limit systems, better in line with observed 60 – 70% covering fraction within the virial radius of $z \sim 2$ quasars.

We are grateful to Dr. Zheng Zheng for allowing us to his program to ACF and CCF, to Dr. Jonathan Richardson and Dr. Yue Shen for sending us the observed ACF and CCF at $z = 1.4$ and $z = 3.2$, and at $z = 0.53$, respectively. We also would like to thank Dr. Zheng for useful discussion. This work is supported in part by grant NASA NNX11AI23G. The Millennium simulation data bases used in this paper and the web application providing online access to them were constructed as part of the activities of the German Astrophysical Virtual Observatory.

REFERENCES

- Abazajian, K. N., Adelman-McCarthy, J. K., Agüeros, M. A., Allam, S. S., Allende Prieto, C., An, D., Anderson, K. S. J., Anderson, S. F., Annis, J., Bahcall, N. A., & et al. 2009, ApJS, 182, 543
- Adelman-McCarthy, J. K., Agüeros, M. A., Allam, S. S., Anderson, K. S. J., Anderson, S. F., Annis, J., Bahcall, N. A., Baldry, I. K., Barentine, J. C., Berlind, A., Bernardi, M., Blanton, M. R., Boroski, W. N., Brewington, H. J., Brinchmann, J., Brinkmann, J., Brunner, R. J., Budavári, T., Carey, L. N., Carr, M. A., Castander, F. J., Connolly, A. J., Csabai, I., Czarapata, P. C., Dalcanton, J. J., Doi, M., Dong, F., Eisenstein, D. J., Evans, M. L.,

Fan, X., Finkbeiner, D. P., Friedman, S. D., Frieman, J. A., Fukugita, M., Gillespie, B., Glazebrook, K., Gray, J., Grebel, E. K., Gunn, J. E., Gurbani, V. K., de Haas, E., Hall, P. B., Harris, F. H., Harvanek, M., Hawley, S. L., Hayes, J., Hendry, J. S., Hennessy, G. S., Hindsley, R. B., Hirata, C. M., Hogan, C. J., Hogg, D. W., Holmgren, D. J., Holtzman, J. A., Ichikawa, S.-i., Ivezić, Ž., Jester, S., Johnston, D. E., Jorgensen, A. M., Jurić, M., Kent, S. M., Kleinman, S. J., Knapp, G. R., Kniazev, A. Y., Kron, R. G., Krzesinski, J., Kuropatkin, N., Lamb, D. Q., Lampeitl, H., Lee, B. C., Leger, R. F., Lin, H., Long, D. C., Loveday, J., Lupton, R. H., Margon, B., Martínez-Delgado, D., Mandelbaum, R., Matsubara, T., McGehee, P. M., McKay, T. A., Meiksin, A., Munn, J. A., Nakajima, R., Nash, T., Neilson, Jr., E. H., Newberg, H. J., Newman, P. R., Nichol, R. C., Nicinski, T., Nieto-Santisteban, M., Nitta, A., O'Mullane, W., Okamura, S., Owen, R., Padmanabhan, N., Pauls, G., Peoples, Jr., J., Pier, J. R., Pope, A. C., Pourbaix, D., Quinn, T. R., Richards, G. T., Richmond, M. W., Rockosi, C. M., Schlegel, D. J., Schneider, D. P., Schroeder, J., Scranton, R., Seljak, U., Sheldon, E., Shimasaku, K., Smith, J. A., Smolčić, V., Snedden, S. A., Stoughton, C., Strauss, M. A., SubbaRao, M., Szalay, A. S., Szapudi, I., Szkody, P., Tegmark, M., Thakar, A. R., Tucker, D. L., Uomoto, A., Vanden Berk, D. E., Vandenberg, J., Vogeley, M. S., Voges, W., Vogt, N. P., Walkowicz, L. M., Weinberg, D. H., West, A. A., White, S. D. M., Xu, Y., Yanny, B., Yocom, D. R., York, D. G., Zehavi, I., Zibetti, S., & Zucker, D. B. 2006, ApJS, 162, 38

Anderson, L., Aubourg, E., Bailey, S., Bizyaev, D., Blanton, M., Bolton, A. S., Brinkmann, J., Brownstein, J. R., Burden, A., Cuesta, A. J., da Costa, L. A. N., Dawson, K. S., de Putter, R., Eisenstein, D. J., Gunn, J. E., Guo, H., Hamilton, J.-C., Harding, P., Ho, S., Honscheid, K., Kazin, E., Kirkby, D., Kneib, J.-P., Labatie, A., Loomis, C., Lupton, R. H., Malanushenko, E., Malanushenko, V., Mandelbaum, R., Manera, M., Maraston, C., McBride, C. K., Mehta, K. T., Mena, O., Montesano, F., Muna, D., Nichol, R. C., Nuza, S. E., Olmstead, M. D., Oravetz, D., Padmanabhan, N., Palanque-Delabrouille, N., Pan, K., Parejko, J., Pâris, I., Percival, W. J., Petitjean, P., Prada, F., Reid, B., Roe, N. A., Ross, A. J., Ross, N. P., Samushia, L., Sánchez, A. G., Schlegel, D. J., Schneider, D. P., Scóccola, C. G., Seo, H.-J., Sheldon, E. S., Simmons, A., Skibba, R. A., Strauss, M. A., Swanson, M. E. C., Thomas, D., Tinker, J. L., Tojeiro, R., Magaña, M. V., Verde, L., Wagner, C., Wake, D. A., Weaver, B. A., Weinberg, D. H., White, M., Xu, X., Yèche, C., Zehavi, I., & Zhao, G.-B. 2012, MNRAS, 427, 3435

Ballantyne, D. R., Shi, Y., Rieke, G. H., Donley, J. L., Papovich, C., & Rigby, J. R. 2006, ApJ, 653, 1070

Bolton, J. S., Becker, G. D., Raskutti, S., Wyithe, J. S. B., Haehnelt, M. G., & Sargent, W. L. W. 2012, MNRAS, 419, 2880

Cen, R. 2011, ApJ, 741, 99

—. 2014, ApJ, 781, 38

Cen, R., & Ostriker, J. P. 1999, ApJ, 514, 1

- Conroy, C., & White, M. 2013, ApJ, 762, 70
- Cowie, L. L., Songaila, A., Hu, E. M., & Cohen, J. G. 1996, AJ, 112, 839
- Davis, M., & Peebles, P. J. E. 1983, ApJ, 267, 465
- Dawson, K. S., Schlegel, D. J., Ahn, C. P., Anderson, S. F., Aubourg, É., Bailey, S., Barkhouser, R. H., Bautista, J. E., Beifiori, A., Berlind, A. A., Bhardwaj, V., Bizyaev, D., Blake, C. H., Blanton, M. R., Blomqvist, M., Bolton, A. S., Borde, A., Bovy, J., Brandt, W. N., Brewington, H., Brinkmann, J., Brown, P. J., Brownstein, J. R., Bundy, K., Busca, N. G., Carithers, W., Carnero, A. R., Carr, M. A., Chen, Y., Comparat, J., Connolly, N., Cope, F., Croft, R. A. C., Cuesta, A. J., da Costa, L. N., Davenport, J. R. A., Delubac, T., de Putter, R., Dhital, S., Ealet, A., Ebelke, G. L., Eisenstein, D. J., Escoffier, S., Fan, X., Filiz Ak, N., Finley, H., Font-Ribera, A., Génova-Santos, R., Gunn, J. E., Guo, H., Haggard, D., Hall, P. B., Hamilton, J.-C., Harris, B., Harris, D. W., Ho, S., Hogg, D. W., Holder, D., Honscheid, K., Huehnerhoff, J., Jordan, B., Jordan, W. P., Kauffmann, G., Kazin, E. A., Kirkby, D., Klaene, M. A., Kneib, J.-P., Le Goff, J.-M., Lee, K.-G., Long, D. C., Loomis, C. P., Lundgren, B., Lupton, R. H., Maia, M. A. G., Makler, M., Malanushenko, E., Malanushenko, V., Mandelbaum, R., Manera, M., Maraston, C., Margala, D., Masters, K. L., McBride, C. K., McDonald, P., McGreer, I. D., McMahon, R. G., Mena, O., Miralda-Escudé, J., Montero-Dorta, A. D., Montesano, F., Muna, D., Myers, A. D., Naugle, T., Nichol, R. C., Noterdaeme, P., Nuza, S. E., Olmstead, M. D., Oravetz, A., Oravetz, D. J., Owen, R., Padmanabhan, N., Palanque-Delabrouille, N., Pan, K., Parejko, J. K., Pâris, I., Percival, W. J., Pérez-Fournon, I., Pérez-Ràfols, I., Petitjean, P., Pfaffenberger, R., Pforr, J., Pieri, M. M., Prada, F., Price-Whelan, A. M., Raddick, M. J., Rebolo, R., Rich, J., Richards, G. T., Rockosi, C. M., Roe, N. A., Ross, A. J., Ross, N. P., Rossi, G., Rubiño-Martin, J. A., Samushia, L., Sánchez, A. G., Sayres, C., Schmidt, S. J., Schneider, D. P., Scóccola, C. G., Seo, H.-J., Shelden, A., Sheldon, E., Shen, Y., Shu, Y., Slosar, A., Smee, S. A., Snedden, S. A., Stauffer, F., Steele, O., Strauss, M. A., Streblyanska, A., Suzuki, N., Swanson, M. E. C., Tal, T., Tanaka, M., Thomas, D., Tinker, J. L., Tojeiro, R., Tremonti, C. A., Vargas Magaña, M., Verde, L., Viel, M., Wake, D. A., Watson, M., Weaver, B. A., Weinberg, D. H., Weiner, B. J., West, A. A., White, M., Wood-Vasey, W. M., Yeche, C., Zehavi, I., Zhao, G.-B., & Zheng, Z. 2013, AJ, 145, 10
- Faucher-Giguere, C.-A., Hopkins, P. F., Keres, D., Muratov, A. L., Quataert, E., & Murray, N. 2014, ArXiv e-prints
- Feldmann, R., Carollo, C. M., & Mayer, L. 2011, ApJ, 736, 88
- Gonçalves, T. S., Steidel, C. C., & Pettini, M. 2008, ApJ, 676, 816
- Hennawi, J. F., Strauss, M. A., Oguri, M., Inada, N., Richards, G. T., Pindor, B., Schneider, D. P., Becker, R. H., Gregg, M. D., Hall, P. B., Johnston, D. E., Fan, X., Burles, S., Schlegel, D. J., Gunn, J. E., Lupton, R. H., Bahcall, N. A., Brunner, R. J., & Brinkmann, J. 2006, AJ, 131, 1

- Hickox, R. C., Mullaney, J. R., Alexander, D. M., Chen, C.-T. J., Civano, F. M., Goulding, A. D., & Hainline, K. N. 2014, ApJ, 782, 9
- Hopkins, A. M., & Beacom, J. F. 2006, ApJ, 651, 142
- Jakobsen, P., Jansen, R. A., Wagner, S., & Reimers, D. 2003, A&A, 397, 891
- Martini, P., & Weinberg, D. H. 2001, ApJ, 547, 12
- McQuinn, M., & Worseck, G. 2014, MNRAS, 440, 2406
- Porciani, C., Magliocchetti, M., & Norberg, P. 2004, MNRAS, 355, 1010
- Prochaska, J. X., Hennawi, J. F., & Simcoe, R. A. 2013, ApJ, 762, L19
- Richards, G. T., Strauss, M. A., Fan, X., Hall, P. B., Jester, S., Schneider, D. P., Vanden Berk, D. E., Stoughton, C., Anderson, S. F., Brunner, R. J., Gray, J., Gunn, J. E., Ivezić, Ž., Kirkland, M. K., Knapp, G. R., Loveday, J., Meiksin, A., Pope, A., Szalay, A. S., Thakar, A. R., Yanny, B., York, D. G., Barentine, J. C., Brewington, H. J., Brinkmann, J., Fukugita, M., Harvanek, M., Kent, S. M., Kleinman, S. J., Krzesiński, J., Long, D. C., Lupton, R. H., Nash, T., Neilson, Jr., E. H., Nitta, A., Schlegel, D. J., & Snedden, S. A. 2006, AJ, 131, 2766
- Richardson, J., Zheng, Z., Chatterjee, S., Nagai, D., & Shen, Y. 2012, ApJ, 755, 30
- Runnoe, J. C., Brotherton, M. S., & Shang, Z. 2012, MNRAS, 422, 478
- Schlegel, D., White, M., & Eisenstein, D. 2009, in ArXiv Astrophysics e-prints, Vol. 2010, astro2010: The Astronomy and Astrophysics Decadal Survey, 314
- Schneider, D. P., Hall, P. B., Richards, G. T., Vanden Berk, D. E., Anderson, S. F., Fan, X., Jester, S., Stoughton, C., Strauss, M. A., SubbaRao, M., Brandt, W. N., Gunn, J. E., Yanny, B., Bahcall, N. A., Barentine, J. C., Blanton, M. R., Boroski, W. N., Brewington, H. J., Brinkmann, J., Brunner, R., Csabai, I., Doi, M., Eisenstein, D. J., Frieman, J. A., Fukugita, M., Gray, J., Harvanek, M., Heckman, T. M., Ivezić, Ž., Kent, S., Kleinman, S. J., Knapp, G. R., Kron, R. G., Krzesinski, J., Long, D. C., Loveday, J., Lupton, R. H., Margon, B., Munn, J. A., Neilson, E. H., Newberg, H. J., Newman, P. R., Nichol, R. C., Nitta, A., Pier, J. R., Rockosi, C. M., Saxe, D. H., Schlegel, D. J., Snedden, S. A., Szalay, A. S., Thakar, A. R., Uomoto, A., Voges, W., & York, D. G. 2005, AJ, 130, 367
- Schneider, D. P., Richards, G. T., Hall, P. B., Strauss, M. A., Anderson, S. F., Boroson, T. A., Ross, N. P., Shen, Y., Brandt, W. N., Fan, X., Inada, N., Jester, S., Knapp, G. R., Krawczyk, C. M., Thakar, A. R., Vanden Berk, D. E., Voges, W., Yanny, B., York, D. G., Bahcall, N. A., Bizyaev, D., Blanton, M. R., Brewington, H., Brinkmann, J., Eisenstein, D., Frieman, J. A., Fukugita, M., Gray, J., Gunn, J. E., Hibon, P., Ivezić, Ž., Kent, S. M., Kron, R. G., Lee, M. G., Lupton, R. H., Malanushenko, E., Malanushenko, V., Oravetz, D., Pan, K., Pier, J. R., Price, III, T. N., Saxe, D. H., Schlegel, D. J., Simmons, A., Snedden, S. A., SubbaRao, M. U., Szalay, A. S., & Weinberg, D. H. 2010, AJ, 139, 2360

- Shen, Y. 2009, ApJ, 704, 89
- Shen, Y., & Kelly, B. C. 2012, ApJ, 746, 169
- Shen, Y., McBride, C. K., White, M., Zheng, Z., Myers, A. D., Guo, H., Kirkpatrick, J. A., Padmanabhan, N., Parejko, J. K., Ross, N. P., Schlegel, D. J., Schneider, D. P., Streblyanska, A., Swanson, M. E. C., Zehavi, I., Pan, K., Bizyaev, D., Brewington, H., Ebelke, G., Malanushenko, V., Malanushenko, E., Oravetz, D., Simmons, A., & Snedden, S. 2013, ApJ, 778, 98
- Shen, Y., Richards, G. T., Strauss, M. A., Hall, P. B., Schneider, D. P., Snedden, S., Bizyaev, D., Brewington, H., Malanushenko, V., Malanushenko, E., Oravetz, D., Pan, K., & Simmons, A. 2011, ApJS, 194, 45
- Shen, Y., Strauss, M. A., Oguri, M., Hennawi, J. F., Fan, X., Richards, G. T., Hall, P. B., Gunn, J. E., Schneider, D. P., Szalay, A. S., Thakar, A. R., Vanden Berk, D. E., Anderson, S. F., Bahcall, N. A., Connolly, A. J., & Knapp, G. R. 2007a, AJ, 133, 2222
- . 2007b, AJ, 133, 2222
- Springel, V., White, S. D. M., Jenkins, A., Frenk, C. S., Yoshida, N., Gao, L., Navarro, J., Thacker, R., Croton, D., Helly, J., Peacock, J. A., Cole, S., Thomas, P., Couchman, H., Evrard, A., Colberg, J., & Pearce, F. 2005, Nature, 435, 629
- Springel, V., White, S. D. M., Tormen, G., & Kauffmann, G. 2001, MNRAS, 328, 726
- Trainor, R., & Steidel, C. C. 2013, ApJ, 775, L3
- Trainor, R. F., & Steidel, C. C. 2012, ApJ, 752, 39
- Treister, E., & Urry, C. M. 2006, ApJ, 652, L79
- White, M., Blanton, M., Bolton, A., Schlegel, D., Tinker, J., Berlind, A., da Costa, L., Kazin, E., Lin, Y.-T., Maia, M., McBride, C. K., Padmanabhan, N., Parejko, J., Percival, W., Prada, F., Ramos, B., Sheldon, E., de Simoni, F., Skibba, R., Thomas, D., Wake, D., Zehavi, I., Zheng, Z., Nichol, R., Schneider, D. P., Strauss, M. A., Weaver, B. A., & Weinberg, D. H. 2011, ApJ, 728, 126
- Worseck, G., Fechner, C., Wisotzki, L., & Dall'Aglio, A. 2007, A&A, 473, 805
- Wyithe, J. S. B., & Loeb, A. 2002, ApJ, 581, 886
- . 2003, ApJ, 595, 614
- Zakamska, N. L., Strauss, M. A., Krolik, J. H., Collinge, M. J., Hall, P. B., Hao, L., Heckman, T. M., Ivezić, Ž., Richards, G. T., Schlegel, D. J., Schneider, D. P., Strateva, I., Vanden Berk, D. E., Anderson, S. F., & Brinkmann, J. 2003, AJ, 126, 2125